Regulation of mitosis by the NIMA kinase involves TINA and its newly discovered partner, An-WDR8, at spindle pole bodies

Kuo-Fang Shen and Stephen A. Osmani
Department of Molecular Genetics and Molecular, Cellular and Developmental Biology Program, Ohio State University, Columbus, OH 43210

ABSTRACT **The NIMA kinase is required for mitotic nuclear pore complex disassembly and potentially controls other mitotic-specific events. To investigate this possibility, we imaged NIMA–green fluorescent protein (GFP) using four-dimensional spinning disk confocal microscopy. At mitosis NIMA-GFP locates to spindle pole bodies (SPBs), which contain Cdk1/cyclin B, followed by Aurora, TINA, and the BimC kinesin. NIMA promotes NPC disassembly in a spatially regulated manner starting near SPBs. NIMA is also required for TINA, a NIMA-interacting protein, to locate to SPBs during initiation of mitosis, and TINA is then necessary for locating NIMA back to SPBs during mitotic progression. To help expand the NIMA-TINA pathway, we affinity purified TINA and found it to uniquely copurify with An-WDR8, a WD40-domain protein conserved from humans to plants. Like TINA, An-WDR8 accumulates within nuclei during G2 but disperses from nuclei before locating to mitotic SPBs. Without An-WDR8, TINA levels are greatly reduced, whereas TINA is necessary for mitotic targeting of An-WDR8. Finally, we show that TINA is required to anchor mitotic microtubules to SPBs and, in combination with An-WDR8, for successful mitosis. The findings provide new insights into SPB targeting and indicate that the mitotic microtubule-anchoring system at SPBs involves WDR8 in complex with TINA.**

Monitoring Editor
Karsten Weis
University of California, Berkeley

Received: Jul 30, 2013
Revised: Sep 24, 2013
Accepted: Oct 11, 2013

INTRODUCTION

In addition to Cdk1, the activity of the NIMA kinase is required for entry into mitosis in *Aspergillus nidulans* (Osmani *et al.*, 1991; Osmani and Ye, 1996). Temperature-sensitive *nimA* alleles, as well as *nimA* deletion or ectopic expression of dominant-negative versions, cause cells to arrest in late G2, indicating an essential role for NIMA in regulating mitotic entry (Oakley and Morris, 1983; Osmani *et al.*, 1987; Lu and Means, 1994; Ye *et al.*, 1998). Moreover, ectopic expression of active NIMA leads to the condensation of chromatin, the disassembly of nuclear pore complexes (NPCs), and mitotic spindle defects, indicating that NIMA plays roles in these mitotic processes (Osmani *et al.*, 1988; De Souza *et al.*, 2004). Experimental evidence suggests that NIMA and related human kinases (see later discussion) play conserved roles in regulating the opening of NPCs via phosphorylation of Nups (Laurell *et al.*, 2011) and the condensation of chromatin, involving phosphorylation of Ser-10 of histone H3 (De Souza *et al.*, 2000). However, it is unclear how NIMA helps to bring about the dramatic structural changes in microtubule dynamics and nuclear structure associated with mitosis.

NIMA is the founding member of the NIMA-related kinase (Nek) family (Moniz *et al.*, 2011; Fry *et al.*, 2012), and ectopic expression of NIMA in fission yeast, *Xenopus*, and human cells promotes mitotic-like events, providing further evidence that NIMA function and substrates are conserved (O'Connell *et al.*, 1994; Lu and Hunter, 1995). Based on the sequence homology within the kinase domain of NIMA and overall domain similarities, multiple Neks have been identified in many eukaryotes (O'Connell *et al.*, 2003). In humans, 11 Neks (Nek1–Nek11) have been identified, and seven of them (Nek1, Nek2, Nek6, Nek7, Nek9–Nek11) have been shown to play roles in

This article was published online ahead of print in MBoC in Press (http://www.molbiolcell.org/cgi/doi/10.1091/mbc.E13-07-0422) on October 23, 2013.

Address correspondence to: Stephen A. Osmani (osmani.2@osu.edu).

Abbreviations used: chRFP, mCherry variant of red fluorescent protein; NE, nuclear envelope; Nek, NIMA-related kinases; NPCs, nuclear pore complexes; SAC, spindle assembly checkpoint; SPBs, spindle pole bodies.

mitotic progression (Fry *et al.*, 1998; Belham *et al.*, 2003; Yissachar *et al.*, 2006; Jeong *et al.*, 2007; Kim *et al.*, 2007; Bahmanyar *et al.*, 2008; Rapley *et al.*, 2008; Melixetian *et al.*, 2009; O'Regan and Fry, 2009; Sorensen *et al.*, 2010; Bertran *et al.*, 2011; Chen *et al.*, 2011; Moniz and Stambolic, 2011; Liu *et al.*, 2013). Similar to NIMA, the protein level and activity of Nek2 are regulated in a cell cycle–specific manner (Fry *et al.*, 1995; Pu and Osmani, 1995; Ye *et al.*, 1995). Nek2 locates to centrosomes, the equivalent structure of the fungal spindle pole body (SPB), and plays an important role in the disjunction of duplicated centrosomes during mitotic entry (Fry *et al.*, 1998; Yang *et al.*, 2006; Bahmanyar *et al.*, 2008). Moreover, Nek6, Nek7, and Nek9 form a signal cascade to regulate the separation of centrosomes via the phosphorylation of Eg5, a BimC kinesin homologue (Belham *et al.*, 2003; Rapley *et al.*, 2008; O'Regan and Fry, 2009; Bertran *et al.*, 2011; Sdelci *et al.*, 2011). Of interest, Nek1, Nek10, and Nek11 also have roles in the DNA damage response (Melixetian *et al.*, 2009; Sorensen *et al.*, 2010; Moniz and Stambolic, 2011; Liu *et al.*, 2013).

Several approaches have been used to understand how mitosis is regulated by NIMA in *A. nidulans*, including extragenic and copy number suppressor screens and yeast two-hybrid analysis (Wu *et al.*, 1998; De Souza *et al.*, 2003; Osmani *et al.*, 2003; Davies *et al.*, 2004; Ukil *et al.*, 2008). Two NPC proteins, SONA and SONB, were identified in the extragenic suppressor screen, and further studies revealed that NPCs undergo partial disassembly during mitosis in *A. nidulans* and that SONB is a potential substrate of NIMA (Wu *et al.*, 1998; De Souza *et al.*, 2003, 2004; Laurell *et al.*, 2011). Taken together, these findings indicate that NIMA regulates mitotic progression via the control of NPC disassembly to allow mitotic regulators to accumulate in nuclei at mitosis.

TINA and TINC are NIMA-interacting proteins identified from yeast two-hybrid screens (Osmani *et al.*, 2003; Davies *et al.*, 2004). TINA locates to SPBs in a cell cycle–specific manner and plays a role in negatively regulating the formation of astral microtubules (Osmani *et al.*, 2003). Similarly Msd1, the *Schizosaccharomyces pombe* TINA homologue, also locates to SPBs during mitosis and plays a role in anchoring mitotic spindle microtubules to SPBs (Toya *et al.*, 2007). However, although TINA and Msd1 share a similar distribution at mitotic SPBs, TINA had not previously been shown to be involved in anchoring microtubules to SPBs during *A. nidulans* mitosis.

RESULTS

NIMA localization during mitosis

Strains containing endogenously green fluorescent protein (GFP)–tagged NIMA (endogenously tagged meaning that the tagged fusion gene is under control of its normal promoter and is the only copy of the gene in the genome) enter and transit mitosis normally and grow and develop like the wild type. In addition, they do not display sensitivity to drugs affecting mitosis (benomyl), S-phase progression (hydroxyurea), or DNA damage (1,2,7,8-diepoxyoctane; unpublished data), indicating that GFP fusion does not affect NIMA function. Using high-resolution, live-cell, spinning-disk four-dimensional (4D) confocal microscopy, we found that NIMA-GFP is excluded from nuclei during interphase and first locates as a distinct focus at the nuclear periphery, a newly identified location, at the G2–M transition. As described later, this focus corresponds to the SPBs. As previously reported (De Souza *et al.*, 2000, 2004), NIMA-GFP then sequentially locates to the nuclear periphery, nuclear chromatin, mitotic spindle, and back to SPBs during exit from mitosis. NIMA-GFP disappears from nuclei as cells progress into G1 (Figure 1A). To ask whether microtubules are required for NIMA's dynamic mitotic localizations, we treated cells with benomyl to depolymerize microtubules (Oakley and Morris, 1981) and monitored them as they entered mitosis. NIMA-GFP still sequentially located first to SPBs and then around the nuclear periphery and back to SPBs, where it remained during spindle assembly checkpoint (SAC)–mediated mitotic arrest (Figure 1B).

NIMA locates first to the spindle pole body at the G2–M transition

Previous studies showed that NIMA locates to SPBs in telophase (De Souza *et al.*, 2000), although NIMA homologues locate earlier to SPBs during mitotic entry (O'Regan *et al.*, 2007). To determine whether the first mitotic NIMA focus corresponds to the SPBs, we generated strains carrying NIMA-GFP in combination with two SPB markers, Sad1–mCherry red fluorescent protein (chRFP; Hagan and Yanagida, 1995; Osmani and Osmani, unpublished data) and GCP3-chRFP (De Souza *et al.*, 2009; Xiong and Oakley, 2009). The colocalization results verify that NIMA-GFP first locates to SPBs at the G2–M transition (Figure 1C and Supplemental Figure S1C). Three-dimensional rotations and single images through *z*-axis series confirm that NIMA-GFP locates to SPBs with Sad1-chRFP during mitotic entry (Supplemental Figures S1A and S2A). We also observed that NIMA-GFP locates back to SPBs in telophase and early G1, as previously reported (De Souza *et al.*, 2000).

Because kinetochores form a cluster at the SPBs in interphase in *A. nidulans*, we asked whether NIMA colocalizes with kinetochores during mitosis. We generated a strain containing NIMA-GFP in combination with NDC80-chRFP (De Souza *et al.*, 2009), a kinetochore marker. NIMA-GFP partially colocalized with NDC80-chRFP upon entry into mitosis (Supplemental Figures S1B and S2B). However, during mitotic kinetochore segregation we did not observe colocalization between NIMA and kinetochores until after anaphase, when the kinetochores had completed segregation to daughter SPBs. This suggests that NIMA-GFP locates to SPBs rather than the clustered kinetochores associated with them during mitotic entry and exit.

The location of NIMA-GFP during mitotic entry in the absence of microtubule function indicates that it is able to first locate to SPBs and then move around the nuclear periphery back to a single focus (Figure 1B). Colocalization of NIMA-GFP with the SPB marker GCP3-chRFP in the absence of microtubules confirms that NIMA-GFP first locates to the SPBs during initiation of mitosis, then locates around the nuclear periphery, and then locates back to the SPBs during mitotic SAC arrest (Supplemental Figure S1D).

NIMA locally promotes NPC disassembly from the SPB region of the nucleus during initiation of mitosis

Several lines of evidence demonstrate that NIMA plays a role in regulating the disassembly of nuclear pores during mitotic entry (Wu *et al.*, 1998; De Souza *et al.*, 2003, 2004; Laurell *et al.*, 2011). If this regulation involves physical association between NIMA and NPCs, there should not be evidence of NPC disassembly before NIMA location to the nuclear periphery. We therefore examined the timing of NIMA localization to the nucleus in relation to NPC disassembly using strains carrying NIMA-GFP in combination with NLS-DsRed or Nup49-chRFP. NLS-DsRed is transported into nuclei in interphase and disperses out of nuclei when nuclear pores are opened during mitosis. We consistently observed NIMA-GFP locating to SPBs as, if not before, NLS-DsRed leaks into the cytoplasm (Figure 2, A and B). NIMA-GFP also appears around the nuclear periphery as the peripheral nuclear pore marker Nup49-chRFP disperses during entry into mitosis (Figure 2, C and D).

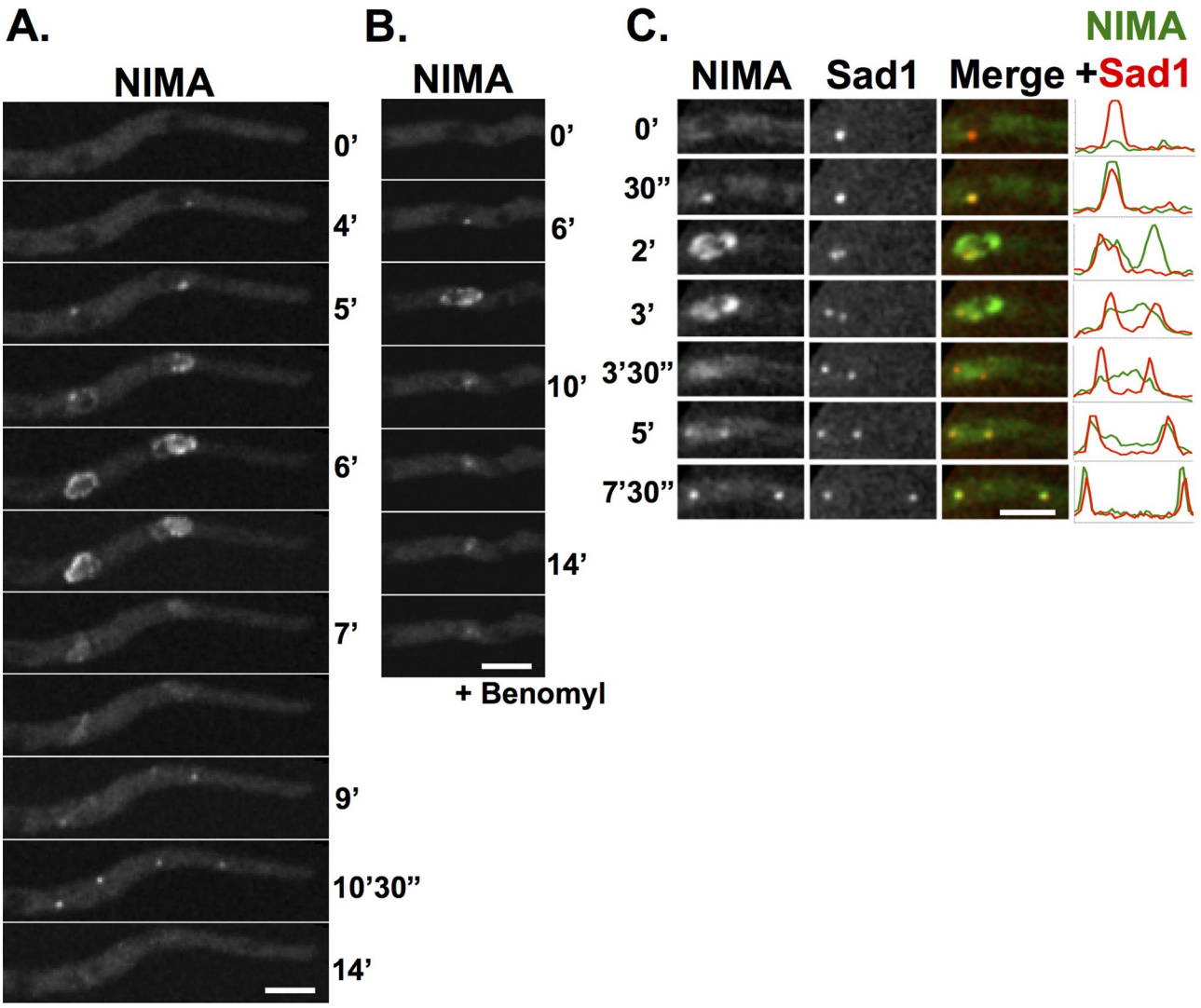

FIGURE 1: NIMA locates to SPBs at the G2–M transition. (A) Live-cell imaging of endogenous NIMA-GFP in strain KF005 shows that it first locates to a newly identified focus at the NE (the SPB; see C) and then sequentially to the nuclear periphery, nuclear interior, spindle, and finally the separated SPBs. (B) Localization of NIMA-GFP (strain KF005) was observed during mitotic entry in the presence of 2.4 μg/ml benomyl to depolymerize microtubules, leading to SAC-mediated mitotic arrest. NIMA still locates to SPBs during mitotic entry and then moves around the nuclear periphery and back to the SPBs. (C) The localization of NIMA-GFP in relation to the SPBs as defined by Sad1-chRFP in strain KF105. NIMA-GFP locates with SPBs in early mitosis and then again at telophase and early G1. The pixel intensity profile reveals that NIMA-GFP colocalizes with Sad1-chRFP at the SPBs during mitotic entry and exit. Bars, 5 μm.

On comparing the data of NIMA-GFP with those for NLS-DsRed or Nup49-chRFP, we noticed that dispersal of NLS-DsRed occurs earlier than that of Nup49-chRFP. This suggests that NIMA targeted to SPBs at the start of mitosis might facilitate local opening of nuclear pores before it spreads around the entire nuclear periphery. If this is the case, it should be possible to observe the release of NLS-DsRed preferentially from the SPB region during initiation of mitosis. Although we were able to see this effect in wild-type (WT) cells (see, e.g., Supplemental Figure S5E, in which NLS-DsRed escapes into the cytoplasm first from the right side of the nucleus), we found that in strains in which NPCs become clustered (Δ*nup133*; Pemberton *et al.*, 1995; Figure 2E), release of NLS-DsRed in the vicinity of the SPBs was more easily detected (Figure 2F). Note in Figure 2F that the cytoplasmic NLS-DsRed signal first appears to the right of the nucleus on the right after NIMA locates to the SPBs, revealing the opening of NPCs from the right side of this nucleus during initiation of mitosis. Using Δ*nup133* mutants, we were also able to formally demonstrate that NIMA-GFP locates to NPCs during entry into mitosis because it locates to the clustered NPCs and not to regions of the nuclear envelope (NE) free of NPCs (Figure 2E).

NIMA localizes to mitotic SPBs before Aurora, TINA, and BimC

During interphase cyclin B accumulates within the nucleoplasm and is concentrated at SPBs before mitosis (Wu *et al.*, 1998; De Souza *et al.*, 2009). Cdk1/cyclin B is required for full mitotic activation of NIMA (Osmani *et al.*, 1991; Ye *et al.*, 1995), and NIMA-3chRFP appears at SPBs to which cyclin B-GFP is already located (Figure 3A). Cyclin B-GFP then disperses from SPBs as cells progress through mitosis (Figure 3A). Because NIMA-3chRFP locates to the SPBs after cyclin B-GFP, we wanted to determine whether Cdk1/cyclin B activity is required for NIMA localization to the SPBs. We found that

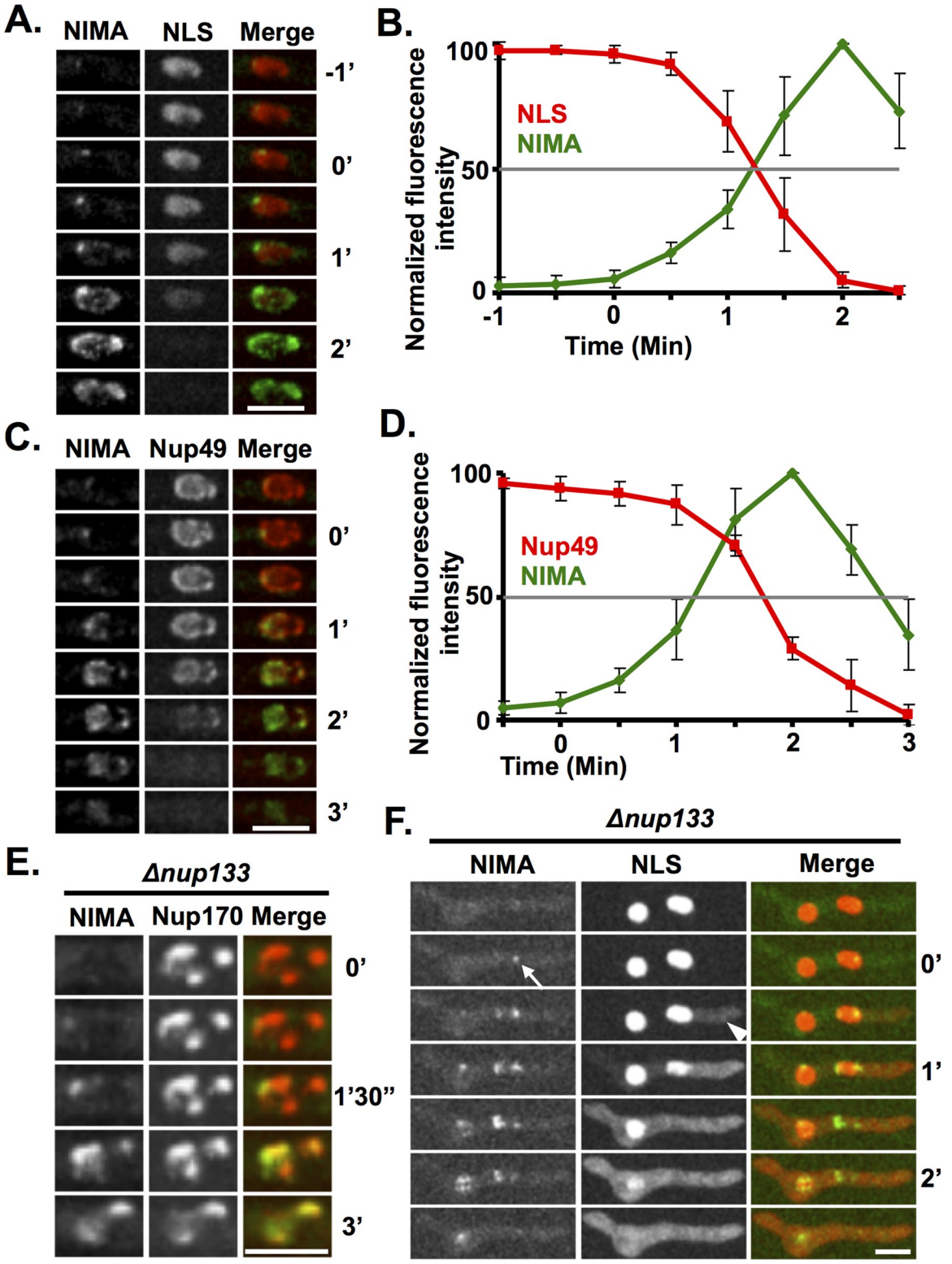

FIGURE 2: NIMA locates to SPBs before mitotic NPC disassembly. (A) The localization of NIMA-GFP in relation to nuclear pore complex disassembly, defined by mitotic NLS-DsRed dispersal, in strain KF033. NIMA-GFP appears at the SPB as NLS-DsRed disperses from the nucleus into the cytoplasm. (B) Quantification of the nuclear signals of NIMA-GFP and NLS-DsRed ($n = 6$). (C) The localization of NIMA-GFP in relation to the disassembly of NPCs defined by Nup49-chRFP was followed in strain KF084. NIMA-GFP spreads around the nuclear periphery as Nup49-chRFP disperses. (D) Quantification of the nuclear signals of NIMA-GFP and Nup49-chRFP ($n = 4$). (E) Live-cell imaging of a *Δnup133* strain (KF450) (in which NPCs cluster) during mitosis after NIMA-GFP and Nup170-chRFP. NIMA-GFP colocalizes with the Nup170-chRFP clusters during mitosis. (F) In a *Δnup133* strain in which NPCs cluster (KF420), NLS-DsRed first starts to disperse from the SPB region (arrowhead) where NIMA-GFP had initially localized (arrow) on the nucleus to the right. NLS-DsRed then disperses completely from both nuclei as mitosis progresses. Bars, 5 μm.

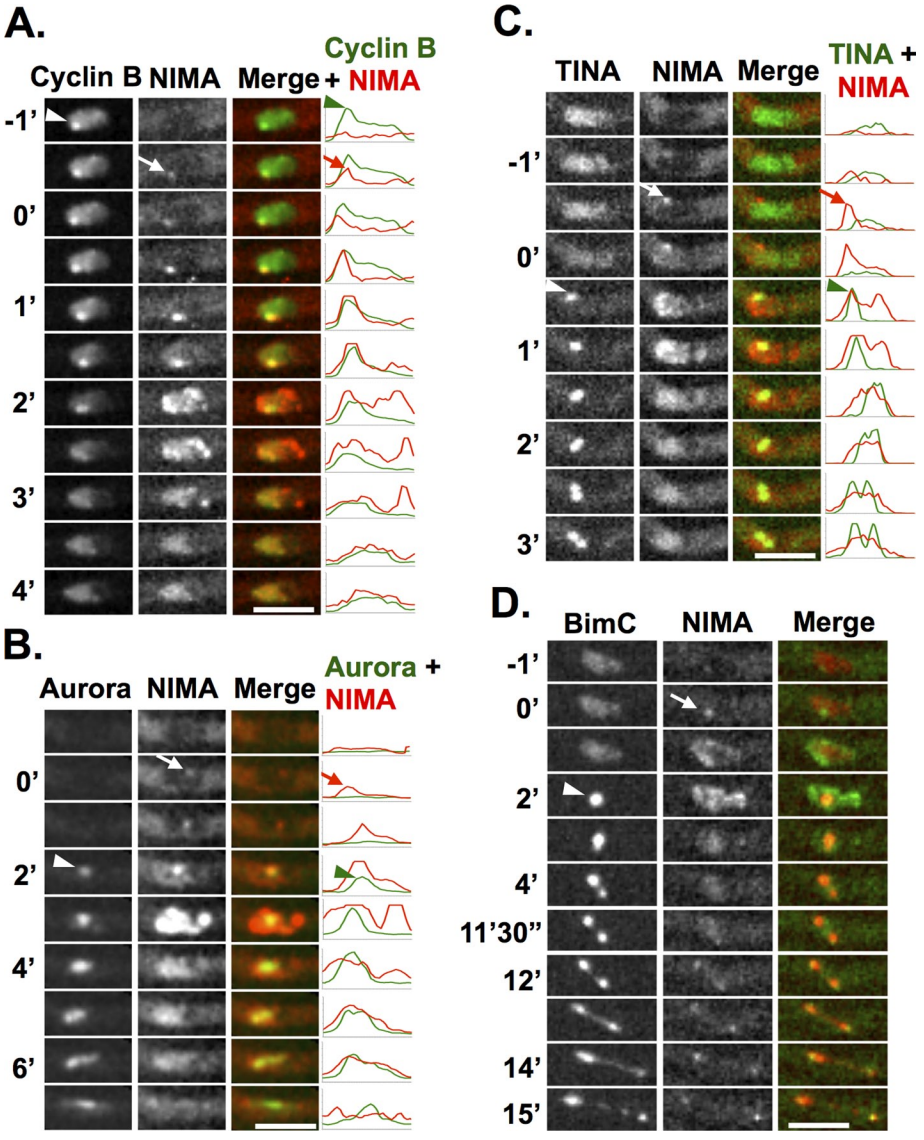

FIGURE 3: NIMA localizes to mitotic SPBs before Aurora, TINA, and BimC. (A) Cyclin B-GFP and NIMA-3chRFP were followed in strain KF126 during mitosis. Cyclin B-GFP is at the SPBs (arrowhead) before NIMA-3chRFP (arrow). The relative pixel intensity line profile indicates that NIMA-3chRFP colocalizes with cyclin B–GFP at the SPBs. (B) Aurora-GFP and NIMA-3chRFP were monitored in strain KF324 during mitosis. Aurora-GFP locates to the SPB region (arrowhead) after NIMA-3chRFP (arrow). The relative pixel intensity line profiles confirm that Aurora-GFP localizes near SPBs after NIMA-3chRFP. (C) TINA-GFP and NIMA-3chRFP were followed in strain KF186 during mitosis. Some TINA-GFP is nuclear, which disperses from the nucleus during mitotic entry. TINA-GFP then appears at the SPBs (arrowhead) after NIMA-3chRFP (arrow), as also revealed by the relative pixel intensity line profile. (D) The location of BimC-chRFP in relation to NIMA-GFP was followed in strain KF129. BimC-chRFP is nuclear before mitosis, and during mitosis it locates (arrowhead) to the forming mitotic spindle after NIMA-GFP has located to SPBs (arrow) and spread around the nucleus. Bars, 5 μm.

Cdk1/cyclin B activity is necessary for NIMA localization to all of its mitotic nuclear structures, including SPBs, using a temperature-sensitive *nimT23*^{Cdc25} strain (blocks mitotic activation of Cdk1; O'Connell *et al.*, 1992) carrying NIMA-GFP and NLS-DsRed, based on G2 block-release experiments (Supplemental Figure S3).

To further define the potential functional relationships between mitotic kinases, we followed the localization of NIMA-3chRFP in relation to the single *A. nidulans* Aurora B–like kinase (Aurora-GFP; De Souza *et al.*, 2013) during entry into mitosis (Figure 3B). Aurora-GFP first locates to the SPB region at mitotic entry and then transitions to its other mitotic locations (De Souza and Osmani, unpublished data; Figure 3B). Time-lapse imaging revealed that Aurora-GFP appears at its mitotic locations after NIMA-3chRFP locates to the SPBs.

TINA, a NIMA-interacting protein identified in a yeast two-hybrid screen, also localizes to the SPB only during mitosis (Osmani *et al.*, 2003). We followed the SPB localization of NIMA-3chRFP in relation to that of TINA-GFP during mitotic entry. We found that, although some TINA-GFP is nuclear before mitosis, surprisingly, this disperses from nuclei during mitotic entry before subsequently locating to SPBs (Figure 3C). The mitotic nuclear release of TINA-GFP and its subsequent SPB location occurs after NIMA-3chRFP locates to the SPBs. To examine whether NIMA is required for the SPB localization of TINA, we generated a *nimA5* strain containing TINA-GFP and shifted it to 42°C to inactivate NIMA. TINA-GFP accumulates and stays in the nucleus and does not disperse into the cytoplasm or locate to the SPBs in the absence of NIMA activity (Supplemental Figure S4, A and B), demonstrating that NIMA is required for TINA nuclear dispersal and localization to the SPBs during mitosis.

BimC, the founding member of the Eg5 family of mitotic kinesins, is required for the separation of duplicated SPBs at the start of mitosis (Enos and Morris, 1990). To follow BimC during mitosis, it was endogenously C-terminally tagged with GFP or chRFP. BimC is nuclear at G2 and concentrates to the forming spindle during mitotic entry (Supplemental Figure S5E) after NIMA has located to the SPBs (Figure 3D). Microtubules were found to be essential for locating BimC to its mitotic locations (Supplemental Figure S5F).

Identification of AN10137 as a TINA-copurifying protein

Because TINA interacts with NIMA and, like its *S. pombe* orthologue Msd1, plays roles at mitotic SPBs, we wanted to expand the regulatory pathway involving these mitotic SPB proteins. We therefore endogenously tagged TINA for affinity purification and used mass spectrometry analysis to identify its interacting partners. Affinity-purified samples from log-phase, G2, or mitotic cell extracts were separated by SDS–PAGE and stained with Coomassie blue to reveal a single high-abundance copurifying protein in each sample (Figure 4A). Mass spectrometry identified the copurifying TINA partner with high sequence coverage as the protein defined by the AN10137 locus at AspGD (www.aspergillusgenome.org/cgi-bin/locus.pl?locus=AN10137&organism=A_nidulans_FGSC_A4; Arnaud *et al.*, 2012; Figure 4B), a highly conserved WD repeat protein of the human WDR8 family (Koshizuka *et al.*, 2001; Figure 4E). We named this protein An-WDR8.

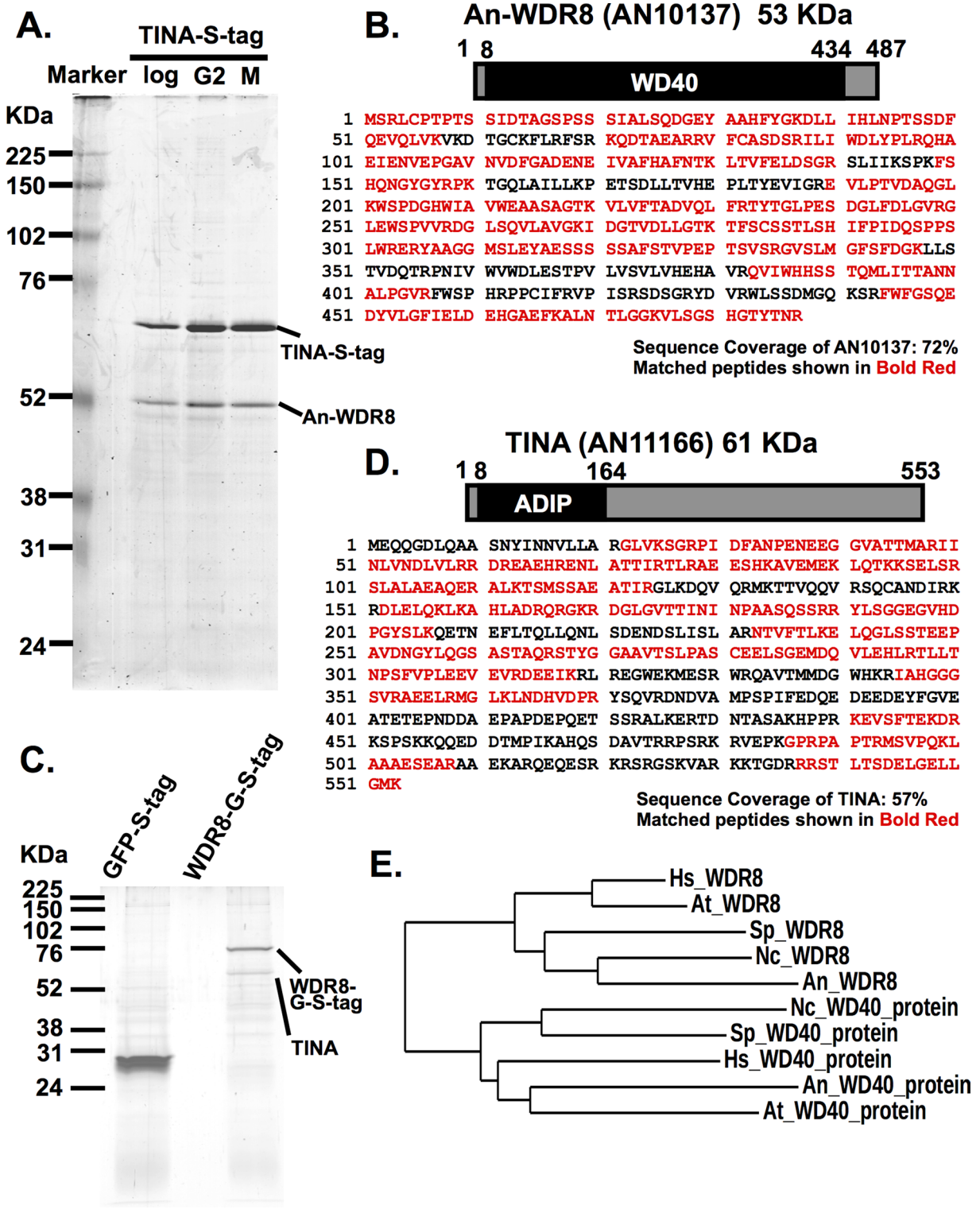

FIGURE 4: Identification of An-WDR8 as a TINA-interacting protein. (A) A *nimA5* strain (KF211) containing endogenously tagged TINA-S-tag was used for affinity purification. After affinity purification, TINA-associated proteins were resolved using SDS–PAGE and visualized by Coomassie blue staining and identified by mass spectrometric analysis. (B) An-WDR8 (AN10137) is a WD40 domain–containing protein identified with 72% sequence coverage. (C) Endogenous GFP-S-tagged An-WDR8 (WDR8-G-S-Tag, strain KF248) was affinity purified, and 1/10 of the purified sample was resolved by SDS–PAGE and visualized after silver staining. The rest of the sample was analyzed by mass spectrometry. (D) WDR8-G-S-tag, but not GFP-S-tag, copurified TINA, which was identified with 57% sequence coverage. (E) An-WDR8–related WD40 proteins were identified by NCBI BLAST, and the second-most related were selected to generate a phylogenic tree. The proteins used in generating the phylogenetic tree were as follows. An, *A. nidulans* (CBF88448.1 and XP_659249.1); At, *Arabidopsis thaliana* (BAE98779.1 and NP_001189659.1); Hs, *Homo sapiens* (CAI14336.1 and 1GXR A); Nc, *Neurospora crassa* (XP_955788.1 and XP_963736.2); and Sp, *S. pombe* (NP_595615.1 and NP_592966.1).

To confirm the interaction between TINA and An-WDR8, we endogenously GFP-S-tagged An-WDR8 (De Souza, Hashmi, and Osmani, unpublished data) at its C-terminus for affinity purification. Affinity purification and mass spectrometry confirmed that TINA copurifies with An-WDR8 (Figure 4, C and D). An-WDR8 is highly conserved, with orthologues apparent in many fungal, plant, and vertebrate species (Figure 4E).

TINA is required for the nuclear and SPB localization of An-WDR8, as well as for NIMA to localize to SPBs during mitotic exit

To follow An-WDR8 localization, we endogenously tagged it at its C-terminus with GFP and followed its localization during the cell cycle from G1 to G2. Time-lapse imaging indicated that although the overall levels of An-WDR8-GFP did not change dramatically, its nuclear levels increased as cells approach mitosis (Figure 5A). A similar increase in nuclear TINA-GFP was also observed (Figure 5C). Quantitation of the ratio of the nuclear signal to that in the cytoplasm revealed that An-WDR8-GFP (Figure 5B) and TINA-GFP (Figure 5D) accumulated in nuclei late in the cell cycle, reaching a maximum just before mitosis.

We next followed An-WDR8 in relationship with TINA during mitosis. This revealed a dynamic pattern in which some An-WDR8 locates to nuclei during interphase (Figure 5, A and B) before dispersing during mitotic entry and relocating to SPBs during mitosis, in a manner identical to TINA (Figure 5E and Supplemental FigureS5, A and C). Given the location of TINA and An-WDR8 to mitotic but not interphase SPBs, we determined whether microtubule depolymerization affected this pattern of TINA and WDR8 localization. After treatment with benomyl to depolymerize microtubules, both TINA-GFP and An-WDR8-GFP are released from nuclei upon entry into mitosis and locate to SPBs as cells delay in mitosis at the SAC arrest point (Supplemental Figure S5, B and D).

To determine whether An-WDR8 is required for TINA localization, we used a Δ*An-wdr8* strain carrying TINA-GFP and NLS-DsRed. Although TINA is in nuclei at G2 and locates to the SPBs during mitosis in the absence of An-WDR8, the signal intensity of TINA-GFP in the nucleus and at SPBs was greatly reduced, being barely detectable above background levels of fluorescence (Figure 5F). Consistent with these microscopy data, TINA-GFP immunoprecipitation (IP)–Western blot analysis revealed that TINA levels are decreased in the absence of An-WDR8 (Figure 5H), indicating that An-WDR8 is required either for normal expression of TINA or for its stability.

To examine whether TINA is necessary for An-WDR8 localization to nuclei at G2 or to the SPBs during mitosis, we generated a Δ*tinA* strain containing An-WDR8-GFP and NLS-DsRed. In the absence of TINA, An-WDR8-GFP does not accumulate in the nucleus during G2 nor does it locate to the SPBs during mitosis (Figure 5G). An-WDR8-GFP IP–Western blot analysis showed that An-WDR8 protein levels in the Δ*tinA* strain are similar those of to the wild-type strain (Figure 5H). To further confirm that TINA is necessary for An-WDR8 localization to SPBs during mitosis, we prolonged mitosis by treating Δ*tinA* cells with benomyl to cause mitotic SAC arrest (De Souza *et al.*, 2011). An-WDR8-GFP does not locate to mitotic SPBs in the absence of TINA during mitotic SAC arrest (Supplemental Figure S6A) but locates normally to the SPBs during mitotic SAC arrest when TINA is reintroduced to Δ*tinA* cells via a genetic cross (Supplemental Figure S6B). These results indicate a multipart relationship in which TINA is required for localization of An-WDR8 to nuclei in G2 and SPBs during mitosis, whereas An-WDR8 is required for normal levels of TINA.

The data presented thus far show that TINA locates to SPBs after NIMA during the G2–M transition and that it stays at the SPBs throughout the remainder of mitosis. We therefore asked whether TINA might be required for NIMA to locate back to the SPBs during mitotic exit. A Δ*tinA* strain containing NIMA-GFP and NLS-DsRed was generated. In the absence of TINA, NIMA-GFP locates normally to the SPBs at the G2–M transition but is unable to locate back to the SPBs during mitotic exit (Figure 6A). NIMA-GFP locates normally to the SPBs in telophase and early G1 when TINA is reintroduced back via a genetic cross (Figure 6B).

The nature of the excessive microtubules caused by lack of TINA during mitosis

The TINA homologue in *S. pombe*, Msd1, is required for anchoring the minus ends of mitotic spindle microtubules to SPBs. Therefore, in the absence of Msd1, mitotic spindle microtubules extend beyond the SPBs, which generates a protruding NE phenotype (Toya *et al.*, 2007). A previous study found that astral microtubules formed from SPBs in the absence of TINA during metaphase delay, a mitotic stage when astral microtubules would normally not be formed. It was concluded that absence of TINA allowed excessive astral microtubule formation because TINA normally plays a negative role in the formation of astral microtubules (Osmani *et al.*, 2003). In this previous study we followed microtubules during a mitotic delay in the absence of TINA and observed microtubules extending beyond the mitotic spindle into the cytoplasm. We concluded that these were astral microtubules seeded from the cytoplasmic face of the SPBs because they physically interacted in the cytoplasm.

Because we did not monitor the NE in our previous study, we asked whether any of the mitotic microtubules extending into the cytoplasmic might be generated via the mechanism proposed in *S. pombe*. To do this, we followed microtubule dynamics using GFP-TubA and the morphology of the NE using chRFP-AN0162, a recently identified inner nuclear membrane (INM) marker that contains a C-terminal transmembrane domain and has similarity to the *S. pombe* INM protein Bqt4 (Osmani and Chemudupati, unpublished data; annotated at AspGD as AN0162, www.aspergillusgenome.org/cgi-bin/locus.pl?dbid=ASPL0000057939). As expected, wild-type cells did not exhibit defects in microtubule dynamics during mitosis, and the NE did not display any abnormal protrusions (Figures 7A and 8A). In a strain lacking TINA, a minor percentage (3%) of mitotic nuclei displayed abnormal protrusions of the NE near SPBs, although most mitoses were normal (Figure 7B). To see the mitotic defects in cells lacking TINA, we previously used a strain carrying a temperature-sensitive allele of the anaphase-promoting complex APC1 subunit (*bimE7*), which causes either metaphase arrest or delay, depending on growth temperature, and causes synthetic growth defects when combined with deletion of *tinA* (Osmani *et al.*, 2003). Growth of *bimE7* mutants at room temperature (22–23°C) did not cause marked mitotic defects (Figure 7C). However, when the deletion of *tinA* was combined with *bimE7*, a significant number of mitotic nuclei (34.6%) displayed microtubule extensions, which caused the NE to protrude away from the SPBs into the cytoplasm (Figure 7, D and D′). This phenotype is very similar, if not identical, to that observed in *S. pombe* when Mds1 is deleted (Toya *et al.*, 2007).

We next asked whether the protrusion of spindle microtubules occurred in the absence of An-WDR8, the aforementioned TINA-interacting protein. In Δ*An-wdr8* mutants (2.0%), Δ*An-wdr8* Δ*tinA* mutants (4.0%), or Δ*An-wdr8 bimE7* mutants (4.0%; Figure 7, E–G) we did not observe a marked increase in the microtubule protrusion phenotype. However, in the triple *bimE7* Δ*tinA* Δ*wdr8* mutant (Figure 7, H and H′) there was an increase in the percentage of mitotic nuclei displaying the NE protrusion phenotype during mitosis to 51.3%. During this analysis we also observed that the *bimE7*

Δ*tinA* Δ*wdr8* mutant strain had a higher frequency of mitotic failure in which nuclei attempted mitosis but failed to generate daughter nuclei (Figure 8B), as well as nuclei in which daughter nuclei remained attached via an NE bridge for an extended period during mitotic exit (Figure 8C). Mitotic defects were greater in the *bimE7* Δ*tinA* Δ*wdr8* strain (28%) than in the *bimE7* Δ*tinA* (0%) or *bimE7* Δ*wdr8* (5.4%) strain, suggesting that TINA and WDR8 have some nonoverlapping mitotic functions.

The microtubules we previously observed in Δ*tinA bimE7* cells had the capacity to physically interact in the cytoplasm between separate mitotic nuclei, indicating that these microtubules are not surrounded by the NE (Osmani *et al.*, 2003). To ask whether there were microtubules forcing the NE out from the SPBs, as well as astral microtubules, we analyzed Δ*tinA bimE7* cells shifted to 32°C to cause a metaphase delay. We could readily detect cells with metaphase-delayed mitotic nuclei displaying both the NE protrusion phenotype and astral microtubules (Supplemental Figure S7A), with some astral microtubules interacting in the cytoplasm, as previously reported (Supplemental Figure S7B). We conclude that in *A. nidulans* lack of TINA, in combination with metaphase delay, leads to both increase in the number of astral microtubules, as we previously reported, and detachment of spindle microtubules from mitotic SPBs, as reported in *S. pombe*.

Finally, we asked whether the microtubules promoting the NE protrusions might contain the microtubule plus end–binding protein EB1 at their ends, suggesting that the responsible microtubules have their plus ends at the distal region of the NE protrusions. For this analysis we used a Δ*tinA* + *bimE7* strain (KF484) grown at 32°C expressing endogenously tagged EB1-GFP (annotated at AspGD as AN2862, www.aspergillusgenome.org/cgi-bin/locus.pl?locus=AN2862) and the NE marker chRFP-AN0162. Of 30 mitotic nuclei examined using live-cell imaging, 28 did not have EB1-GFP located at any time during the imaging in the distal region of the protrusion but did have EB1-GFP located within the mitotic spindle region itself. This indicates that the majority of microtubules forcing the NE away from the spindle pole body region are not oriented with their plus ends protruding past the SPBs.

DISCUSSION

The order of events at SPBs during mitosis

The localization of NIMA to duplicated SPBs during mitotic entry led us to test the timing of other events occurring at mitotic SPBs in relation to NIMA. We expected to see NIMA appear at SPBs before other proteins if NIMA had a role in regulating their location and functions. In terms of mitotic kinases, we found that Cdk1/cyclin B first locates to SPBs, followed by NIMA and then Aurora. This suggests that Cdk1/cyclin B could act as a regulator of NIMA in a spatially controlled manner at SPBs after its mitotic activation by the $NimT^{Cdc25}$ phosphatase. Consistent with this possibility, Cdk1/cyclin B mitotic activation is required for SPB localization of NIMA, and these kinases colocalize transiently during mitotic entry. In addition, it was previously shown that Cdk1/cyclin B is required to fully activate mitotic NIMA kinase activity (Ye *et al.*, 1995). Collectively these insights suggest a model in which NIMA is activated by Cdk1/cyclin B at SPBs, after Cdk1 is activated by $NimT^{Cdc25}$, for NIMA to help promote separation of SPBs and then transition onto NPCs to promote their disassembly, followed by mitotic spindle formation. One potential downstream target of NIMA is Aurora because it locates to its mitotic nuclear locations only after SPB location, and presumably activation, of NIMA.

BimC is a kinesin required for bipolar spindle formation, and its mammalian homologue, Eg5, has been identified as a substrate of Nek6 (Rapley *et al.*, 2008). Phosphorylation of Eg5 at Ser-1033 by Nek6 is necessary for normal spindle formation (Rapley *et al.*, 2008). We find that NIMA locates to SPBs before BimC, and the mitotic localization of BimC depends on microtubules and the activity of NIMA. The requirement for NIMA for BimC locations most likely reflects the necessity for NIMA activity to promote spindle formation.

Nek2, a NIMA-related kinase, plays a key role in regulating the disjunction of mitotic centrosomes (Fry *et al.*, 1998; Bahe *et al.*, 2005; Bahmanyar *et al.*, 2008). The localization of NIMA at duplicated SPBs during initiation of mitosis indicates that NIMA could play a similar role to Nek2 in separation of duplicated SPBs in *A. nidulans*. In addition to a role in the separation of duplicated SPBs, NIMA might also play roles in the nucleation of spindle microtubules, as it is required for this key aspect of mitosis, and NIMA-related kinases, such as Fin1 in fission yeast and Nek6, Nek7, and Nek9 in humans, function in spindle formation (Grallert and Hagan, 2002; Krien *et al.*, 2002; van Hemert *et al.*, 2002; Sdelci *et al.*, 2011). Our data showing that NIMA locates to SPBs and is required for separation of duplicated SPBs and formation of spindle microtubules indicate that these roles for NIMA and related kinases are conserved.

NIMA also locates to SPBs during later stages of mitosis, and this location depends on TINA. Because NIMA is required for SPB loading of TINA, it therefore seeds the mechanism for its own return to SPBs. As will be discussed later, TINA is required for normal anchoring of spindle microtubules to SPBs, raising the intriguing possibility that this function might involve targeting of NIMA to SPBs after NIMA first targets TINA to SPBs.

NIMA and the spatially regulated disassembly of NPCs during mitosis

A. nidulans undergoes partially open mitosis in which peripheral nuclear pore complex proteins disperse throughout the cell during mitosis (De Souza *et al.*, 2004; Liu *et al.*, 2009). We showed here that NIMA locates specifically to NPCs and not the nuclear envelope, using the clustered NPC phenotype of Δ*nup133* mutants. Of importance, NIMA first locates to SPBs at mitotic entry, and we saw that NLS-DsRed begins to disperse into the cytoplasm from the region of the nucleus near the SPBs only after NIMA locates to the SPBs. This indicates that NIMA has the ability to promote the disassembly of NPCs in a spatially regulated manner starting near SPBs. This in theory might allow tubulin into nuclei first in the vicinity of SPBs to facilitate mitotic spindle formation.

Roles of TINA and An-WDR8 during mitotic progression

We used TINA affinity purification to identify An-WDR8 as a new TINA-interacting protein. An-WDR8 is a WD40 repeat–domain protein present in organisms ranging from fission yeast to humans and plants. Similar to TINA, An-WDR8 locates to the nucleus in G2, disperses during mitotic entry, and then subsequently locates to SPBs during mitosis. Why these proteins are first released from nuclei to locate to the cytoplasm instead of directly locating to SPBs from the nucleus during mitotic entry is an interesting question. One possibility is that TINA and An-WDR8 have a function in the cytoplasm during mitotic entry, perhaps to help prevent the formation of microtubules from the cytoplasmic side of SPBs during the early stages of mitosis. In addition, we found that the localization of An-WDR8 to the nucleus and to SPBs depends on TINA, whereas An-WDR8 is required for maintaining the protein levels of TINA. Given the conservation of An-WDR8 and it role in maintaining TINA protein level at SPBs, An-WDR8 homologues might play similar roles at SPBs or their functional equivalents. In this regard we note that the human orthologue WDR8 (also

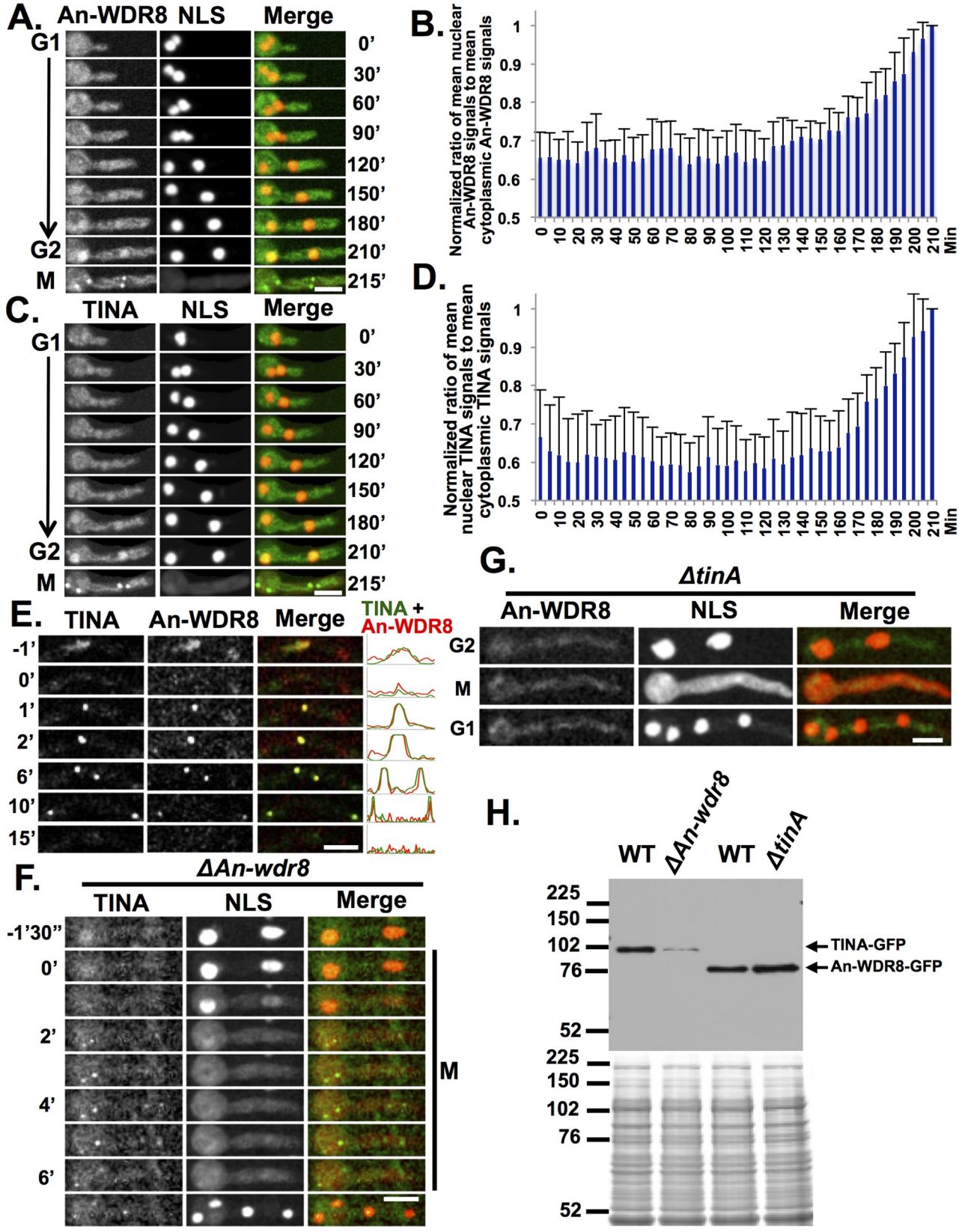

FIGURE 5: TINA is required for An-WDR8 location to interphase nuclei and mitotic SPBs. (A) Localization of An-WDR8-GFP during interphase progression in strain KF280. The nuclear An-WDR8-GFP signal is low in G1 but increases as cells progress toward mitosis. (B) Ratio of mean nuclear An-WDR8-GFP signal to mean cytoplasmic An-WDR8-GFP signal plotted against time in interphase ($N = 10$). (C) Localization of TINA-GFP during interphase progression in strain KF278. The nuclear TINA-GFP signal is low in G1 but increases as cells progress toward mitosis. (D) Ratio of mean nuclear TINA-GFP signal to mean cytoplasmic TINA-GFP signal ($N = 10$). In A–D, time 210 is the time point just before mitosis,

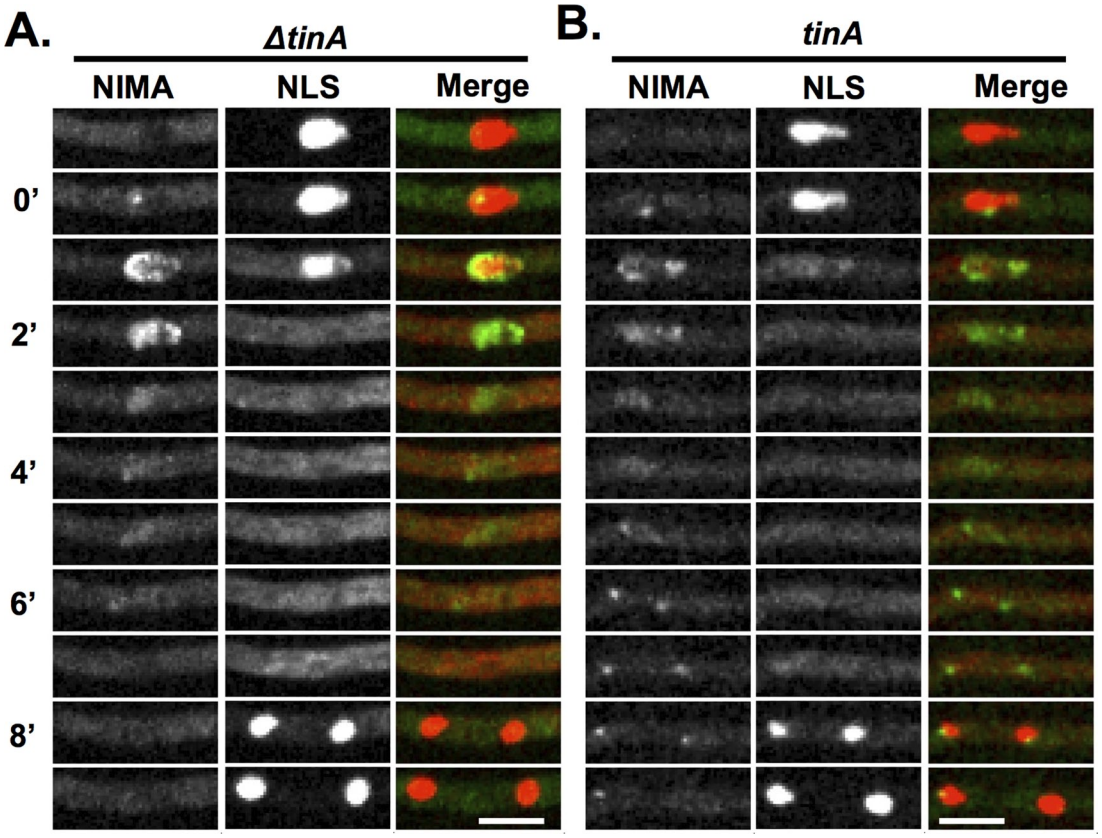

FIGURE 6: TINA is required for NIMA to locate back to SPBs during mitotic exit. (A) A Δ*tinA* strain (KF334) was used to follow NIMA-GFP and NLS-DsRed during mitosis. In the absence of TINA, NIMA-GFP locates normally to duplicated SPBs and then the nuclear periphery during early mitosis but cannot locate back to the separated SPBs during later stages of mitosis. (B) The Δ*tinA* strain (KF334) was crossed to reintroduce TINA. This strain (KF345) was imaged during mitosis, showing that NIMA-GFP can locate back to the SPBs during mitotic exit in the presence of reintroduced TINA. Bars, 5 μm.

termed WRP73; Koshizuka *et al.*, 2001) has been identified as a constituent of centrosomes, functional equivalents of fungal SPBs (Jakobsen *et al.*, 2011), indicative of a common function. In terms of its function, given that deletion of An-WDR8 causes reduction in the levels TINA, it could be predicted to play a role in the expression of TINA or be required for stabilizing TINA. Because An-WDR8 was recently identified via TAP-tagged affinity purification of the ubiquitin-like protein Nedd8, which is covalently linked to target proteins via a process termed neddylation and is involved in regulation of ubiquitin-mediated proteolysis pathways (Petroski and Deshaies, 2005; Higa *et al.*, 2006; von Zeska Kress *et al.*, 2012), we favor a model in which An-WDR8 helps prevent degradation of TINA.

We did not previously use a nuclear membrane marker to determine whether the microtubules formed beyond the SPB into the cytoplasm in Δ*tinA* cells could represent protrusion of the minus ends of spindle microtubules dislodged from SPBs as shown for cells lacking Msd1, the TINA orthologue of *S. pombe* (Toya *et al.*, 2007). We completed this experiment to reveal that, as in *S. pombe*, lack of TINA causes mitotic microtubules to extend beyond SPBs, causing protrusions of the NE into the cytoplasm beyond SPBs. We also confirmed that additional astral microtubules extend beyond mitotic SPBs that do not displace the NE. Thus TINA is required for negatively regulating the formation of astral microtubules as previously proposed in *A. nidulans*, as well as for anchoring spindle microtubules to the SPBs as defined in *S. pombe*. Although An-WDR8 plays a role in controlling the levels of TINA, because deletion of both causes more penetrant mitotic defects than deletion of TINA alone, An-WDR8 might affect other proteins beyond TINA. These

defined as when NLS-DsRed is dispersed from nuclei. (E) An-WDR8-chRFP is seen to colocalize with TINA-GFP at G2 and during mitosis in strain KF328. Both TINA-GFP and An-WDR8-chRFP locate to the nucleus in G2 and are released from the nucleus during initiation of mitosis. Subsequently, they both locate to SPBs during mitosis and then disappear from SPBs in G1. (F) A Δ*An-wdr8* strain (KF327) carrying TINA-GFP was followed during mitosis. In the absence of An-WDR8, TINA-GFP still locates to the nucleus at G2 and SPBs during mitosis, but the signal intensity of TINA-GFP is markedly decreased to just above background levels. (G) A Δ*tinA* strain (KF302) carrying An-WDR8-GFP and NLS-DsRed was imaged during mitosis. An-WDR8-GFP failed to accumulate in the nucleus during G2 or locate to SPBs in the absence of TINA. (H) GFP-tagged TINA or An-WDR8 was immunoprecipitated with an anti-GFP antibody and resolved by SDS–PAGE. Proteins were detected by immunoblot using an anti-GFP antibody, revealing that An-WDR8 is required for normal TINA protein levels. Coomassie blue staining of whole-cell extracts (bottom) shows that equal amounts of protein were used for the purifications. Bars, 5 μm.

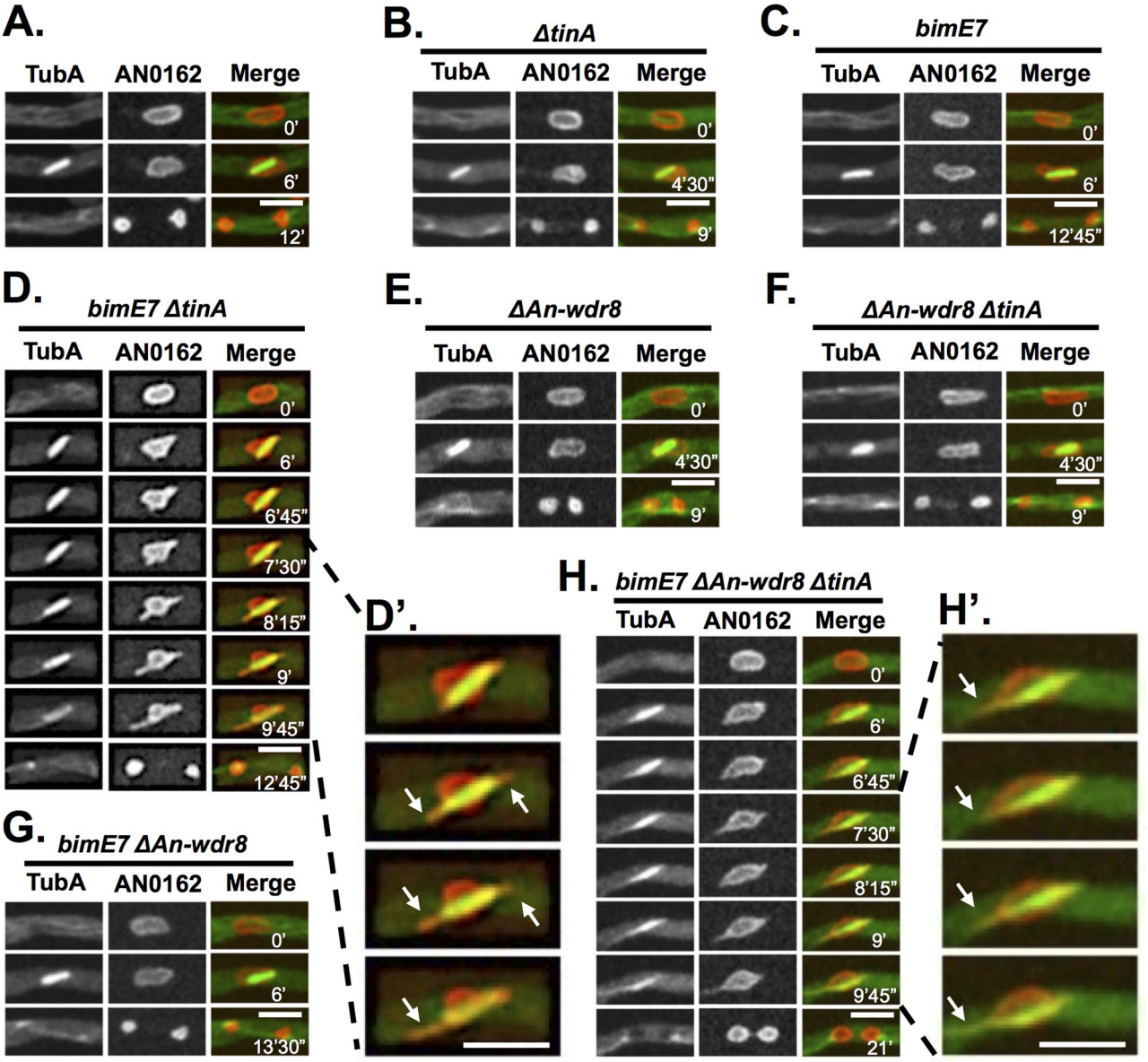

FIGURE 7: TINA is required for anchoring spindle microtubules to SPBs during mitosis. Strains (A) WT (KF439), (B) Δ*tinA* (KF440), (C) *bimE7* (KF438), (D) Δ*tinA bimE7* (KF433), (E) ΔAn-*wdr8* (KF452), (F) ΔAn-*wdr8* Δ*tinA* (KF453), (G) ΔAn-*wdr8 bimE7* (KF466), and (H) ΔAn-*wdr8* Δ*tinA bimE7* (KF451) expressing TubA-GFP tubulin and chRFP-AN0162 (an inner nuclear membrane marker) were followed during mitosis at 23°C. Strain KF452 also contains GCP3-chRFP in addition to TubA-GFP and chRFP-AN0162. Nuclear membrane protrusions occur due to defects in anchoring spindle microtubules to SPBs in Δ*tinA bimE7* (9 of 26 showed nuclear membrane protrusion) and ΔAn-*wdr8* Δ*tinA bimE7* (39 of 76 showed nuclear membrane protrusion) strains, indicated by arrows in the expanded views in D′ and H′. Bars, 5 μm.

findings extend the pathway required to anchor microtubules to mitotic SPBs involving TINA/Msd1 and the γ-tubulin complex (Toya *et al.*, 2007) to also include the conserved WDR8 protein, which interacts with TINA and similarly locates specifically to SPBs during mitosis.

MATERIALS AND METHODS

Media and classic genetic techniques used for *A. nidulans* have been previously described (Pontecorvo *et al.*, 1953; Todd *et al.*, 2007a,b). Strains used in this study are listed in Table 1. S-Tag-, GFP-, and chRFP-tagged strains were generated using standard techniques (Yang *et al.*, 2004; Nayak *et al.*, 2006; Szewczyk *et al.*, 2006; Liu *et al.*, 2009). The GFP-S-Tag dual localization and affinity tag construct used to purify An-WDR8 was generated by De Souza *et al.* (unpublished data). None of the S-Tag-, GFP-, GFP-S-Tag-, or chRFP-tagged versions of proteins conferred growth defects, indicating that they are functional. S-Tag affinity purification was carried out according to the protocol previously published (Liu *et al.*, 2010). Immunoprecipitation and Western blotting were carried out according to previously described standard procedures (Osmani *et al.*, 2006). Mass spectrometry analysis was completed at the Ohio State University Campus Chemical Instrument Center (Columbus, OH).

To C-terminally endogenously tag NIMA with three tandem copies of a red fluorescent protein (3xchRFP), were introduced *Sal*I and *Xho*I restriction enzyme sites at either end into six fragments (the 3′ region of *nimA*, GA5-chRFP, chRFP, chRFP-stop, and *pyroA* and the 3′ untranslated region [UTR] of *nimA*) by PCR. Six sequential cloning steps were completed in the following order: *Sal*I-GA5-chRFP-*Xho*I

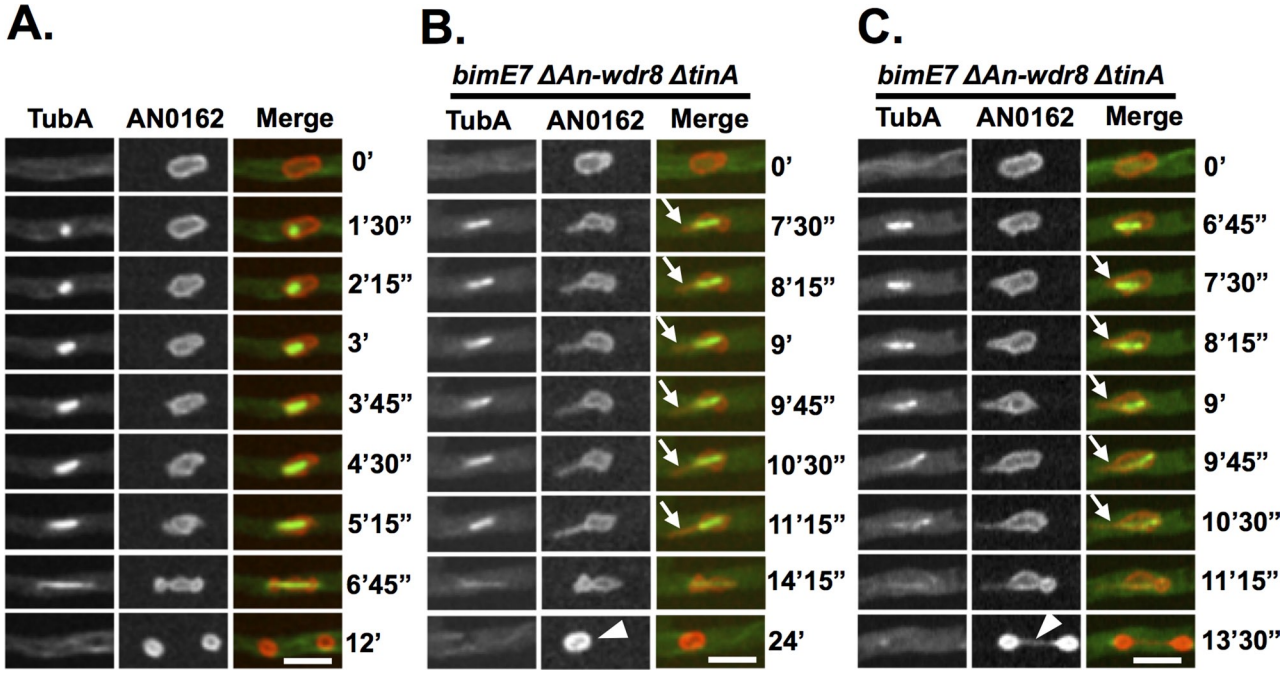

FIGURE 8: TINA and An-WDR8 are required for successful mitosis. Cells carrying TubA-GFP and chRFP-AN0162 were followed during mitosis at 23°C. (A) During normal mitosis in strain KF439, G2 nuclei divide successfully into two G1 nuclei. During abnormal mitosis in a strain carrying *bimE7* and ΔAn-*wdr8* Δ*tinA* (KF451), mitotic nuclei either fail to divide into two G1 nuclei (B) or remain linked by a nuclear envelope bridge (C) (25 of 89 showed abnormal mitosis). Arrows indicate nuclear membrane protrusions. Arrowhead in B indicates that a single nucleus remains after mitosis. Arrowhead in C indicates that a nuclear envelope linkage remains between G1 daughter nuclei. Bars, 5 μm.

Strain	Genotype (all strains also carry *veA1*)	Strain	Genotype (all strains also carry *veA1*)
KF005	*nimA*-GFP::*pyrG*^{AF}; (*pyrG89*); *pyroA4*; Δ*nKuA*::*argB*; (*argB2*); *sE15*; *nirA14*; *wA3*; *fwA1*; *chaA1*	KF202	*tinA*-GFP::*pyrG*^{AF}; (*pyrG89*); *pyroA4*; *sE15*; *nirA14*; Δ*nKuA*::*argB*; (*argB2*); *wA3*; *fwA1*; *chaA1*
KF032	*nimA*-GFP::*pyrG*^{AF}; *pyroA4*; Δ*yA*::NLS-DsRed; *nimT23*; Δ*nKuA*::*argB*; (*argB2?*)	KF211	*tinA*-Stag::*pyrG*^{AF}; (*pyrG89*); *argB2*; *nirA14?*; *nimA5*; *wA3*; *fwA1*; *chaA1*
KF033	*nimA*-GFP::*pyrG*^{AF}; *pyroA4*; Δ*yA*::NLS-DsRed; Δ*nKuA*::*argB*; (*argB2*); *nirA14?*; *sE15?*	KF221	*tinA*-GFP::*pyrG*^{AF}; *argB2*; *nirA14?*; *sE15?*; *nimA5*
KF043	*nimA*-GFP::*pyrG*$^{AF;}$ *gcp3*-chRFP::*ribo*$^{AF;}$ Δ*nKuA*::*argB*; *pyroA4*; *nirA14?*; *sE15?*; *wA3*	KF248	*An-wdr8*-GFP-S-tag::*pyrG*^{AF}; (*pyrG89*); *pyroA4*; *nirA14*; *sE15*; Δ*nKuA*::*argB*; (*argB2*); *wA3*; *fwA1*; *chaA1*
KF045	*nimA*-GFP::*pyrG*^{AF}; *ndc80*-chRFP::*pyroA*^{AF}; *argB2*; *nirA14?*; *sE15?*; *wA3*	KF278	*tinA*-GFP::*pyroA*^{AF}; *pyroA4*; *pyrG89*; Δ*yA*::NLS-DsRed; Δ*nKuA*::*argB*; (*argB2*)
KF084	*nimA*-GFP::*pyrG*^{AF}; *nup49*-chRFP::*pyroA*^{AF}; Δ*nKuA*::*argB*; *nirA14?*; *wA3*	KF280	*An-wdr8*-GFP::*pyroA*^{AF}; Δ*yA*::NLS-DsRed; Δ*nKuA70* ::*argB* (*argB2*); *pyrG89*; (*pyroA4*)
KF105	*nimA*-GFP::*pyrG*^{AF}; (*pyrG89*); *sad1*-chRFP::*pyroA*; (*pyroA4*); *nirA14*; *sE15*; Δ*nKuA*::*argB*; (*argB2*); *wA3*	KF302	*An-wdr8*-GFP::*pyroA*^{AF}; Δ*yA*::NLS-DsRed; Δ*nKuA*::*argB* (*argB2*); Δ*tinA*::*pyrG*^{AF}; (*pyrG89*); (*pyroA4*)
KF126	*nimA*-3chRFP::*pyroA*^{AF}; *nimE*-GFP::*pyrG*^{AF}; *riboB2*; Δ*nKuA*::*argB*; (*argB2 ?*); *wA3*	KF308	*bimC*-GFP::*pyrG*^{AF}; (*pyrG89*); *argB2*; *pyroA4*; Δ*yA*::NLS-DsRed; *nirA14?*
KF129	*nimA*-GFP::*pyrG*^{AF}; (*pyrG89*); *bimC*-chRFP::*pyroA*^{AF}; (*pyroA4*); *nirA14*; *sE15*; Δ*nKuA*::*argB*; (*argB2*); *wA3*; *fwA1*; *chaA1*	KF324	*nimA*-3chRFP::*pyroA*^{AF}; *An-Aurora*-GFP::*pyrG*^{AF}; (*pyrG89*); *argB2*; *fwA1*
KF144	*nimA*-3chRFP::*pyroA*^{AF}*bimC*-GFP::*pyrG*^{AF}; *pyrG89*; *pyroA4*; *nirA14*; *sE15*; Δ*nKuA*::*argB*; (*argB2*); *wA3*; *fwA1*; *chaA1*	KF327	Δ*An-wdr8*::*pyrG*^{AF}; *tinA*-GFP::*pyroA*^{AF}; (*pyroA4*); (*pyrG89*); Δ*yA*::NLS-DsRed; Δ*nKuA*::*argB*; (*argB2*)
KF186	*tinA*-GFP::*pyrG*^{AF}; (*pyrG89*); *nimA*-3chRFP::*pyroA*^{AF}; (*pyroA4*); *nirA14*; *sE15*; Δ*nKuA*::*argB*; (*argB2*); *wA3*; *fwA1*; *chaA1*	KF328	*An-wdr8*-chRFP::*pyroA*; (*pyroA4*); *tinA*-GFP::*pyrG*^{AF}; (*pyrG89*); *sE15*; *nirA14*; Δ*nKuA*::*argB*; (*argB2*); *wA3*; *fwA1*; *chaA1*
		KF334	*nimA*-GFP::*pyrG*^{AF}; Δ*tinA*::*pyroA*^{AF}; (*pyroA4*); Δ*yA*::NLS-DsRed; Δ*nKuA*::*argB*; (*argB2*); *nirA14?*

TABLE 1: Strains.

Continues

Strain	Genotype (all strains also carry *veA1*)	Strain	Genotype (all strains also carry *veA1*)
KF345	*nimA*-GFP::*pyrG*^{AF}; *pyroA4*; Δ*yA*::NLS-DsRed; Δ*nKuA::argB*; *(argB2?)*; *nirA14?*; *sE15?*	KF450	Δ*Nup133::pyrG*^{AF}; *nimA*-GFP::*pyrG*^{AF} *or nimA*-GFP::*pyroA*^{AF}; *argB2*; *Nup170*-chRFP::*pyroA*^{AF}; *nirA14?*; *sE15?*; *chaA2*
KF351	*pyrG89*; *tinA*-GFP::*pyroA*^{AF}; *(pyroA4)*; Δ*nKuA::argB*; *(argB2)*; *gcp3*-chRFP::*ribo*$^{AF;}$ *nirA14?*	KF451	*bimE7*; *tinA*Δ::*pyrG/Zeo cassette*; *(pyrG89)*; chRFP-*AN0162*; GFP-*tubA*; Δ*nKuA::arg*; *(argB2?)*; Δ*AN10137::pyroA*; *(pyroA4)*
KF353	*pyrG89*; *An-wdr8*-GFP::*pyroA*^{AF}; *(pyroA4)*; *gcp3*-chRFP::*ribo*^{AF}; Δ*nKuA::argB*; *(argB2)*	KF452	*pyrG89*; GFP-*tubA*; chRFP-*AN0162*; *gcp3*-chRFP::*ribo*^{AF}; Δ*nKuA::argB*; *(argB2)*; Δ*An-wdr8::pyroA*; *(pyroA4)*
KF411	*pyrG89*; *An-wdr8*-GFP::*pyroA*^{AF}; *(pyroA4)*; Δ*nKuA::argB*; *(argB2)*; Δ*yA*::NLS-DsRed	KF453	*tinA*Δ::*pyrG/Zeo cassette*; *(pyrG89)*; chRFP-*AN0162*; GFP-*tubA*; Δ*nKuA::argB*; *(argB2)*; Δ*An-wdr8::pyroA*; *(pyroA4)*
KF420	Δ*nup133::pyrG*^{AF}; *(pyrG89)*; *nimA*-GFP::*pyroA*^{AF}; *argB2*; Δ*yA*::NLS-DsRed; *nirA14?*; *sE15?*	KF466	*bimE7*; *tubA*-GFP; chRFP-*AN0162*; Δ*An-wdr8::pyrG*^{AF}; *(pyrG89)*; Δ*yA*::NLS-DsRed; *pyroA4*; Δ*nKuA::argB*; *nirA14?*; *sE15?*
KF433	*bimE7*; *tinA*Δ::*pyrG/Zeo cassette*; *(pyrG89)*; chRFP-*AN0162*; GFP- *tubA*; *pabaA1*; *wA3*	KF484	*bimE7*; *tinA*Δ::*pyrG/Zeo cassette*; *(pyrG89)*; *EB1*-GFP::*pyroA*^{AF}; chRFP-*AN0162*; Δ*nKuA::arg*; *(argB2)*; *(pyroA4)*
KF438	*bimE7*; *pyrG89*; *pyroA4*; Δ*nKuA::argB*; *(argB2?)*; chRFP-*AN0162*; GFP-*TubA*		
KF439	*pyrG89*; chRFP-*AN0162*; GFP-*tubA*; *pabaA1*; Δ*nKuA::argB*; *(argB2?)*		
KF440	*tinA*Δ::*pyrG/Zeo cassette*; *(pyrG89)*; chRFP-*AN0162*; GFP-*TubA*; Δ*nKuA::argB*; *(argB2)*; *pyroA4*; *pabaA1*		

A question mark indicates that the marker may or may not be present in the strain.

TABLE 1: Strains. Continued

into *Sal*I and *Xho*I-cut pBluescript SK (+). This plasmid was cut with *Xho*I and the *Sal*I-chRFP-*Xho*I fragment cloned into it. After determination of the correct orientation, this plasmid was cut with *Xho*I and the *Sal*I-chRFP-stop-*Xho*I fragment cloned into it. After determination of the correct orientation, this plasmid was cut with *Xho*I and the *Sal*I- *pyroA-Xho*I fragment cloned into it. After determination of the correct orientation, this plasmid was cut with *Sal*I and the *Sal*I-3′ region of *nimA-Xho*I fragment cloned into it. After determination of the correct orientation, this plasmid was cut with *Xho*I and the *Sal*I-3′ UTR of *nimA-Xho*I fragment cloned into it. After determination of the correct orientation, the inserted fragment of this plasmid was cut out using *Sal*I and *Xho*I and transformed into strain SO451.

For live-cell imaging, we used inverted microscopes (Nikon, Melville, NY) configured with UltraVIEW spinning disk confocal systems controlled by UltraVIEW or Volocity software (Perkin Elmer, Waltham, MA) and using a Nikon Plan Apo 60×/1.40 numerical aperture oil objective. All confocal images presented are maximum-intensity projections unless indicated. ImageJ software (National Institutes of Health, Bethesda, MD) was used for image analysis, and quantitation was completed as described previously (De Souza *et al*., 2011). For quantification of the mean signal intensity of TINA and An-WDR8 from G1 to G2, Volocity software was used to measure the mean signals of nuclear TINA, cytoplasmic TINA, nuclear An-WDR8, and cytoplasmic AnWDR8. The mean ratio of nuclear TINA to cytoplasmic TINA and the mean ratio of nuclear AnWDR8 to cytoplasmic An-WDR8 of the images collected just before mitosis were quantitated. Graphs were plotted using Excel software (Microsoft, Redmond, WA), and error bars indicate mean ± SD.

WDR8-like proteins were identified using BLAST analysis (National Center for Biotechnology Information [NCBI]; www.ncbi.nlm.nih.gov) and AspGD (www.aspergillusgenome.org; Arnaud *et al*., 2012). The amino acid sequence alignment for WDR8-like proteins was done using MUSCLE (Edgar, 2004), and the phylogenic tree was generated at www.phylogeny.fr (Dereeper *et al*., 2008).

ACKNOWLEDGMENTS

We thank all members of the Osmani laboratory for their help and input into this work, particularly Colin P.C. De Souza and Jennifer Larson for discussions and critical reading of the manuscript. We also thank Colin P.C. De Souza for use of the Aurora-GFP strain and the GFP-S-Tag construct he developed and Mahesh Chemudupati for the chRFP-AN0162 strain. We also thank Kari Green at the Ohio State University Campus Chemical Instrument Center for mass spectrometry data analysis. This work was supported by a grant from the National Institutes of Health (GM042564) to S.A.O.

REFERENCES

Arnaud MB *et al.* (2012). The *Aspergillus* Genome Database (AspGD): recent developments in comprehensive multispecies curation, comparative genomics and community resources. Nucleic Acids Res 40, D653–D659.

Bahe S, Stierhof YD, Wilkinson CJ, Leiss F, Nigg EA (2005). Rootletin forms centriole-associated filaments and functions in centrosome cohesion. J Cell Biol 171, 27–33.

Bahmanyar S, Kaplan DD, Deluca JG, Giddings TH Jr, O'Toole ET, Winey M, Salmon ED, Casey PJ, Nelson WJ, Barth AI (2008). beta-Catenin is a Nek2 substrate involved in centrosome separation. Genes Dev 22, 91–105.

Belham C, Roig J, Caldwell JA, Aoyama Y, Kemp BE, Comb M, Avruch J (2003). A mitotic cascade of NIMA family kinases. Nercc1/Nek9 activates the Nek6 and Nek7 kinases. J Biol Chem 278, 34897–34909.

Bertran MT, Sdelci S, Regue L, Avruch J, Caelles C, Roig J (2011). Nek9 is a Plk1-activated kinase that controls early centrosome separation through Nek6/7 and Eg5. EMBO J 30, 2634–2647.

Chen Y, Chen CF, Riley DJ, Chen PL (2011). Nek1 kinase functions in DNA damage response and checkpoint control through a pathway independent of ATM and ATR. Cell Cycle 10, 655–663.

Davies JR, Osmani AH, De Souza CP, Bachewich C, Osmani SA (2004). Potential link between the NIMA mitotic kinase and nuclear membrane fission during mitotic exit in *Aspergillus nidulans.* Eukaryot Cell 3, 1433–1444.

Dereeper A *et al.* (2008). Phylogeny.fr: robust phylogenetic analysis for the non-specialist. Nucleic Acids Res 36, W465–W469.

De Souza CP, Hashmi SB, Nayak T, Oakley B, Osmani SA (2009). Mlp1 acts as a mitotic scaffold to spatially regulate spindle assembly checkpoint proteins in *Aspergillus nidulans*. Mol Biol Cell 20, 2146–2159.
De Souza CP, Hashmi SB, Osmani AH, Andrews P, Ringelberg CS, Dunlap JC, Osmani SA (2013). Functional analysis of the *Aspergillus nidulans* kinome. PLoS One 8, e58008.
De Souza CP, Hashmi SB, Yang X, Osmani SA (2011). Regulated inactivation of the spindle assembly checkpoint without functional mitotic spindles. EMBO J 30, 2648–2661.
De Souza CP, Horn KP, Masker K, Osmani SA (2003). The SONB(NUP98) nucleoporin interacts with the NIMA kinase in *Aspergillus nidulans*. Genetics 165, 1071–1081.
De Souza CP, Osmani AH, Hashmi SB, Osmani SA (2004). Partial nuclear pore complex disassembly during closed mitosis in *Aspergillus nidulans*. Curr Biol 14, 1973–1984.
De Souza CP, Osmani AH, Wu LP, Spotts JL, Osmani SA (2000). Mitotic histone H3 phosphorylation by the NIMA kinase in *Aspergillus nidulans*. Cell 102, 293–302.
Edgar RC (2004). MUSCLE: multiple sequence alignment with high accuracy and high throughput. Nucleic Acids Res 32, 1792–1797.
Enos AP, Morris NR (1990). Mutation of a gene that encodes a kinesin-like protein blocks nuclear division in *A. nidulans*. Cell 60, 1019–1027.
Fry AM, Mayor T, Meraldi P, Stierhof YD, Tanaka K, Nigg EA (1998). C-Nap1, a novel centrosomal coiled-coil protein and candidate substrate of the cell cycle-regulated protein kinase Nek2. J Cell Biol 141, 1563–1574.
Fry AM, O'Regan L, Sabir SR, Bayliss R (2012). Cell cycle regulation by the NEK family of protein kinases. J Cell Sci 125, 4423–4433.
Fry AM, Schultz SJ, Bartek J, Nigg EA (1995). Substrate specificity and cell cycle regulation of the Nek2 protein kinase, a potential human homolog of the mitotic regulator NIMA of *Aspergillus nidulans*. J Biol Chem 270, 12899–12905.
Grallert A, Hagan IM (2002). *Schizosaccharomyces pombe* NIMA-related kinase, Fin1, regulates spindle formation and an affinity of Polo for the SPB. EMBO J 21, 3096–3107.
Hagan I, Yanagida M (1995). The product of the spindle formation gene sad1 +associates with the fission yeast spindle pole body and is essential for viability. J Cell Biol 129, 1033–1047.
Higa LA, Wu M, Ye T, Kobayashi R, Sun H, Zhang H (2006). CUL4-DDB1 ubiquitin ligase interacts with multiple WD40-repeat proteins and regulates histone methylation. Nat Cell Biol 8, 1277–1283.
Jakobsen L *et al*. (2011). Novel asymmetrically localizing components of human centrosomes identified by complementary proteomics methods. EMBO J 30, 1520–1535.
Jeong Y, Lee J, Kim K, Yoo JC, Rhee K (2007). Characterization of NIP2/centrobin, a novel substrate of Nek2, and its potential role in microtubule stabilization. J Cell Sci 120, 2106–2116.
Kim S, Lee K, Rhee K (2007). NEK7 is a centrosomal kinase critical for microtubule nucleation. Biochem Biophys Res Commun 360, 56–62.
Koshizuka Y, Ikegawa S, Sano M, Nakamura K, Nakamura Y (2001). Isolation, characterization, and mapping of the mouse and human WDR8 genes, members of a novel WD-repeat gene family. Genomics 72, 252–259.
Krien MJ, West RR, John UP, Koniaras K, McIntosh JR, O'Connell MJ (2002). The fission yeast NIMA kinase Fin1p is required for spindle function and nuclear envelope integrity. EMBO J 21, 1713–1722.
Laurell E, Beck K, Krupina K, Theerthagiri G, Bodenmiller B, Horvath P, Aebersold R, Antonin W, Kutay U (2011). Phosphorylation of Nup98 by multiple kinases is crucial for NPC disassembly during mitotic entry. Cell 144, 539–550.
Liu HL, De Souza CP, Osmani AH, Osmani SA (2009). The three fungal transmembrane nuclear pore complex proteins of *Aspergillus nidulans* are dispensable in the presence of an intact An-Nup84–120 complex. Mol Biol Cell 20, 616–630.
Liu HL *et al*. (2010). Single-step affinity purification for fungal proteomics. Eukaryot Cell 9, 831–833.
Liu S, Ho CK, Ouyang J, Zou L (2013). Nek1 kinase associates with ATR-ATRIP and primes ATR for efficient DNA damage signaling. Proc Natl Acad Sci USA 110, 2175–2180.
Lu KP, Hunter T (1995). Evidence for a NIMA-like mitotic pathway in vertebrate cells. Cell 81, 413–424.
Lu KP, Means AR (1994). Expression of the noncatalytic domain of the NIMA kinase causes a G2 arrest in *Aspergillus nidulans*. EMBO J 13, 2103–2113.
Melixetian M, Klein DK, Sorensen CS, Helin K (2009). NEK11 regulates CDC25A degradation and the IR-induced G2/M checkpoint. Nat Cell Biol 11, 1247–1253.
Moniz L, Dutt P, Haider N, Stambolic V (2011). Nek family of kinases in cell cycle, checkpoint control and cancer. Cell Div 6, 18.
Moniz LS, Stambolic V (2011). Nek10 mediates G2/M cell cycle arrest and MEK autoactivation in response to UV irradiation. Mol Cell Biol 31, 30–42.
Nayak T, Szewczyk E, Oakley CE, Osmani A, Ukil L, Murray SL, Hynes MJ, Osmani SA, Oakley BR (2006). A versatile and efficient gene-targeting system for *Aspergillus nidulans*. Genetics 172, 1557–1566.
Oakley BR, Morris NR (1981). A beta-tubulin mutation in *Aspergillus nidulans* that blocks microtubule function without blocking assembly. Cell 24, 837–845.
Oakley BR, Morris NR (1983). A mutation in *Aspergillus nidulans* that blocks the transition from interphase to prophase. J Cell Biol 96, 1155–1158.
O'Connell MJ, Krien MJ, Hunter T (2003). Never say never. The NIMA-related protein kinases in mitotic control. Trends Cell Biol 13, 221–228.
O'Connell MJ, Norbury C, Nurse P (1994). Premature chromatin condensation upon accumulation of NIMA. EMBO J 13, 4926–4937.
O'Connell MJ, Osmani AH, Morris NR, Osmani SA (1992). An extra copy of nimEcyclinB elevates pre-MPF levels and partially suppresses mutation of nimTcdc25 in *Aspergillus nidulans*. EMBO J 11, 2139–2149.
O'Regan L, Blot J, Fry AM (2007). Mitotic regulation by NIMA-related kinases. Cell Div 2, 25.
O'Regan L, Fry AM (2009). The Nek6 and Nek7 protein kinases are required for robust mitotic spindle formation and cytokinesis. Mol Cell Biol 29, 3975–3990.
Osmani AH, Davies J, Liu HL, Nile A, Osmani SA (2006). Systematic deletion and mitotic localization of the nuclear pore complex proteins of *Aspergillus nidulans*. Mol Biol Cell 17, 4946–4961.
Osmani AH, Davies J, Oakley CE, Oakley BR, Osmani SA (2003). TINA interacts with the NIMA kinase in *Aspergillus nidulans* and negatively regulates astral microtubules during metaphase arrest. Mol Biol Cell 14, 3169–3179.
Osmani AH, McGuire SL, Osmani SA (1991). Parallel activation of the NIMA and p34cdc2 cell cycle-regulated protein kinases is required to initiate mitosis in *A. nidulans*. Cell 67, 283–291.
Osmani SA, May GS, Morris NR (1987). Regulation of the mRNA levels of nimA, a gene required for the G2-M transition in *Aspergillus nidulans*. J Cell Biol 104, 1495–1504.
Osmani SA, Pu RT, Morris NR (1988). Mitotic induction and maintenance by overexpression of a G2-specific gene that encodes a potential protein kinase. Cell 53, 237–244.
Osmani SA, Ye XS (1996). Cell cycle regulation in *Aspergillus* by two protein kinases. Biochem J 317(Pt 3), 633–641.
Pemberton LF, Rout MP, Blobel G (1995). Disruption of the nucleoporin gene NUP133 results in clustering of nuclear pore complexes. Proc Natl Acad Sci USA 92, 1187–1191.
Petroski MD, Deshaies RJ (2005). Function and regulation of cullin-RING ubiquitin ligases. Nat Rev Mol Cell Biol 6, 9–20.
Pontecorvo G, Roper JA, Hemmons LM, Macdonald KD, Bufton AW (1953). The genetics of *Aspergillus nidulans*. Adv Genet 5, 141–238.
Pu RT, Osmani SA (1995). Mitotic destruction of the cell cycle regulated NIMA protein kinase of *Aspergillus nidulans* is required for mitotic exit. EMBO J 14, 995–1003.
Rapley J, Nicolas M, Groen A, Regue L, Bertran MT, Caelles C, Avruch J, Roig J (2008). The NIMA-family kinase Nek6 phosphorylates the kinesin Eg5 at a novel site necessary for mitotic spindle formation. J Cell Sci 121, 3912–3921.
Sdelci S, Bertran MT, Roig J (2011). Nek9, Nek6, Nek7 and the separation of centrosomes. Cell Cycle 10, 3816–3817.
Sorensen CS, Melixetian M, Klein DK, Helin K (2010). NEK11: linking CHK1 and CDC25A in DNA damage checkpoint signaling. Cell Cycle 9, 450–455.
Szewczyk E, Nayak T, Oakley CE, Edgerton H, Xiong Y, Taheri-Talesh N, Osmani SA, Oakley BR (2006). Fusion PCR and gene targeting in *Aspergillus nidulans*. Nat Protoc 1, 3111–3120.
Todd RB, Davis MA, Hynes MJ (2007a). Genetic manipulation of *Aspergillus nidulans*: heterokaryons and diploids for dominance, complementation and haploidization analyses. Nat Protoc 2, 822–830.
Todd RB, Davis MA, Hynes MJ (2007b). Genetic manipulation of *Aspergillus nidulans*: meiotic progeny for genetic analysis and strain construction. Nat Protoc 2, 811–821.
Toya M, Sato M, Haselmann U, Asakawa K, Brunner D, Antony C, Toda T (2007). Gamma-tubulin complex-mediated anchoring of spindle microtubules to spindle-pole bodies requires Msd1 in fission yeast. Nat Cell Biol 9, 646–653.

Ukil L, Varadaraj A, Govindaraghavan M, Liu HL, Osmani SA (2008). Copy number suppressors of the *Aspergillus nidulans* nimA1 mitotic kinase display distinctive and highly dynamic cell cycle-regulated locations. Eukaryot Cell 7, 2087–2099.

van Hemert MJ, Lamers GE, Klein DC, Oosterkamp TH, Steensma HY, van Heusden GP (2002). The *Saccharomyces cerevisiae* Fin1 protein forms cell cycle-specific filaments between spindle pole bodies. Proc Natl Acad Sci USA 99, 5390–5393.

von Zeska Kress MR, Harting R, Bayram O, Christmann M, Irmer H, Valerius O, Schinke J, Goldman GH, Braus GH (2012). The COP9 signalosome counteracts the accumulation of cullin SCF ubiquitin E3 RING ligases during fungal development. Mol Microbiol 83, 1162–1177.

Wu L, Osmani SA, Mirabito PM (1998). A role for NIMA in the nuclear localization of cyclin B in *Aspergillus nidulans*. J Cell Biol 141, 1575–1587.

Xiong Y, Oakley BR (2009). In vivo analysis of the functions of gamma-tubulin-complex proteins. J Cell Sci 122, 4218–4227.

Yang J, Adamian M, Li T (2006). Rootletin interacts with C-Nap1 and may function as a physical linker between the pair of centrioles/basal bodies in cells. Mol Biol Cell 17, 1033–1040.

Yang L, Ukil L, Osmani A, Nahm F, Davies J, De Souza CP, Dou X, Perez-Balaguer A, Osmani SA (2004). Rapid production of gene replacement constructs and generation of a green fluorescent protein-tagged centromeric marker in *Aspergillus nidulans*. Eukaryot Cell 3, 1359–1362.

Ye XS, Fincher RR, Tang A, Osmani AH, Osmani SA (1998). Regulation of the anaphase-promoting complex/cyclosome by bimAAPC3 and proteolysis of NIMA. Mol Biol Cell 9, 3019–3030.

Ye XS, Xu G, Pu RT, Fincher RR, McGuire SL, Osmani AH, Osmani SA (1995). The NIMA protein kinase is hyperphosphorylated and activated downstream of p34cdc2/cyclin B: coordination of two mitosis promoting kinases. EMBO J 14, 986–994.

Yissachar N, Salem H, Tennenbaum T, Motro B (2006). Nek7 kinase is enriched at the centrosome, and is required for proper spindle assembly and mitotic progression. FEBS Lett 580, 6489–6495.